This is the author's version of an article that has been published in this journal. Changes were made to this version by the publisher prior to publication.
The final version of record is available at http://dx.doi.org/10.1109/TVT.2017.2787204

An Extension of the κ-μ Shadowed Fading Model: Statistical Characterization and Applications

Pablo Ramirez-Espinosa, F. Javier Lopez-Martinez, Jose F. Paris, Michel D. Yacoub, Eduardo Martos-Naya

***Abstract*—We here introduce an extension and natural generalization of both the κ-μ shadowed and the classical Beckmann fading models: the Fluctuating Beckmann (FB) fading model. This new model considers the clustering of multipath waves on which the line-of-sight (LoS) components randomly fluctuate, together with the effect of in-phase/quadrature power imbalance in the LoS and non-LoS components. Thus, it unifies a variety of important fading distributions as the one-sided Gaussian, Rayleigh, Nakagami-m, Rician, κ-μ, η-μ, η-κ, Beckmann, Rician shadowed and the κ-μ shadowed distribution. The chief probability functions of the FB fading model, namely probability density function, cumulative distribution function and moment generating function are derived. The second-order statistics such as the level crossing rate and the average fade duration are also analyzed. These results can be used to derive some performance metrics of interest of wireless communication systems operating over FB fading channels.**

***Index Terms*—Fading channels, Beckmann, Rayleigh, Nakagami-m, Rician, κ-μ, Rician shadowed, κ-μ shadowed.**

I. Introduction

In wireless environments, the radio signal is affected by a number of random phenomena including reflection (both specular and diffuse), diffraction, and scattering as they travel from transmitter to receiver, giving rise to the so-called multipath propagation. At the receiver, the resulting signal appears as a linear combination of the multipath waves, each of which with their own amplitudes and phases. When the number of paths is sufficiently large, the complex baseband signal can be regarded as Gaussian because of the Central Limit Theorem (CLT). Depending on the choice of the parameters characterizing this complex Gaussian random variable, namely the mean and variance of the in-phase and quadrature components, different fading models emerge: Rayleigh (zero-mean and equal variances), Hoyt (zero-mean and unequal variances) and Rice (non-zero mean, equal variances), which are perhaps the most popular fading models arising from the CLT assumption [1, 2].

Copyright (c) 2015 IEEE. Personal use of this material is permitted. However, permission to use this material for any other purposes must be obtained from the IEEE by sending a request to pubs-permissions@ieee.org.

P. Ramirez-Espinosa, F. J. Lopez-Martinez, J. F. Paris and E. Martos-Naya are with Departmento de Ingeniería de Comunicaciones, Universidad de Malaga - Campus de Excelencia Internacional Andalucía Tech., Malaga 29071, Spain. E-mail: {pre,fjlopezm,paris,eduardo}@ic.uma.es. This work has been funded by the Consejería de Economía, Innovación, Ciencia y Empleo of the Junta de Andalucía, the Spanish Government and the European Fund for Regional Development FEDER (projects P2011-TIC-7109, P2011-TIC-8238, and TEC2014-57901-R).

M. D. Yacoub is with the Wireless Technology Laboratory, School of Electrical and Computer Engineering, University of Campinas, Campinas 13083-970, Brazil. E-mail michel@decom.fee.unicamp.br.

The most general case (i.e. unequal means and variances for the in-phase and quadrature components) was considered by Beckmann [3, 4] when characterizing the scattering from rough surfaces. However, its greater flexibility comes at the price of an increased mathematical complexity; in fact, its chief probability functions, Probability Density Function (PDF) and Cumulative Distribution Function (CDF) are known to be given in infinite-series form expression [5], as opposed to Rayleigh, Hoyt and Rician models. Other models characterizing the joint effects of imbalances in the mean and variance between in-phase and quadrature components whose PDF and CDF are given in infinite-series form are the so-called η-κ [6, 7] and the very recently proposed α-η-κ-μ [8].

In order to provide a better statistical characterization of the received radio signal in multipath environments, some alternative models have been proposed as generalizations of classical Rayleigh, Hoyt and Rician. By means of considering the effect of clustering of multipath waves, two new fading models arise [9]: the η-μ fading model as a generalization of Hoyt model, well-suited for non line-of-sight (NLoS) propagation environments, and the κ-μ fading model as a generalization of Rice model in line-of-sight[1] (LoS) scenarios. These models have become of widespread use in the recent years because of their flexibility and relatively simple mathematical tractability, as their chief probability functions; PDF, CDF and Moment Generating Function (MGF), are given in closed-form [9–11]. Besides, both models also include the versatile and popular Nakagami-m model as particular case [12].

A further generalization of these models was introduced in [13] and [14] under the name of κ-μ shadowed fading distribution. This new distribution provides an additional degree of freedom compared to the κ-μ distribution by allowing the LoS component to randomly fluctuate. Notably, the κ-μ shadowed fading model includes both the κ-μ and η-μ models [15] as special cases, as well as the Rician shadowed fading model [16]. Thus, most popular fading models in the literature for LoS and NLoS conditions are unified under the umbrella of the κ-μ shadowed fading channel model. This greater flexibility does not come at the price of an increased mathematical complexity; in fact, in some cases its PDF and CDF admit a representation in terms of a finite number of powers and exponentials, thus becoming even as tractable as the Nakagami-m distribution [17].

Even though the κ-μ shadowed fading model succeeds on capturing different propagation phenomena such as clustering

[1]Line-of-sight is used here to mean the more precise phenomenon concerning the presence of dominant components.

Copyright (c) 2018 IEEE. Personal use is permitted. For any other purposes, permission must be obtained from the IEEE by emailing pubs-permissions@ieee.org.

This is the author's version of an article that has been published in this journal. Changes were made to this version by the publisher prior to publication.
The final version of record is available at http://dx.doi.org/10.1109/TVT.2017.2787204

and LoS fluctuation, it fails when it comes to accounting for the effect of power imbalance in the LoS and NLoS components as originally considered by Beckmann [3, 4]. Motivated by this issue, in this paper we introduce an extended κ-μ shadowed fading model which effectively captures such propagation conditions. This new model can be regarded as a generalization of the original fading model in [13], but also as a generalization of Beckmann fading model by also including the effects of clustering and LoS fluctuation. For this reason, and for the sake of notational brevity, we deem appropriate to name it as the Fluctuating Beckmann (FB) fading model (or equivalently, fading distribution).

The FB model includes as special cases an important set of fading distributions as the one-sided Gaussian, Rayleigh, Nakagami-m, Rician, κ-μ, η-μ, η-κ, Beckmann, Rician shadowed and the κ-μ shadowed distributions.

Interestingly, the CDF and PDF of the FB fading model are given in terms of a well-known function in the context of communication theory, having a functional form similar to the original κ-μ shadowed fading model. The randomization of the LoS component allows for including an additional degree of freedom when compared to the Beckmann model. We provide a full statistical characterization of the FB fading model in terms of its first-order statistics (PDF, CDF and MGF) and second-order statistics (level crossing rate and average fade duration), and then exemplify its applicability to wireless performance analysis.

The remainder of this paper is structured as follows: the physical model of the FB fading distribution is described in Section II. In Section III the PDF, CDF and MGF of this distribution are derived. Then, in Section IV the level crossing rate (LCR) and average fade duration (AFD) are computed. These statistical results are then used to derive some performance metrics of interest in Section V. Finally, the main conclusions are outlined in Section VI.

II. Physical model

The physical model of the FB distribution arises as a generalization of the physical model of the κ-μ shadowed distribution [13, 18]. The received radio signal is built out of a superposition of radio waves grouped into a number of clusters of waves, and the received signal power W can be expressed in terms of the in-phase and quadrature components of the received signal affected by fading as follows

$$W = \sum_{i=1}^{\mu} \left(X_i + p_i\xi\right)^2 + \left(Y_i + q_i\xi\right)^2, \tag{1}$$

where μ is a natural number indicating the number of clusters, X_i and Y_i are mutually independent Gaussian random processes with $E[X_i] = E[Y_i] = 0$, $E[X_i^2] = \sigma_x^2$, $E[Y_i^2] = \sigma_y^2$, p_i and q_i are real numbers and ξ is[2] a Nakagami-m distributed random variable with shape parameter m and $E[\xi^2] = 1$ which accounts for the fluctuation of the LoS component.

As opposed to the κ-μ shadowed fading model, we here consider that X_i and Y_i can have different variances. Thus, the effect of power imbalance in the diffuse components associated to non-LoS propagation is considered. Similarly, we also assume that the power of the LoS components can be imbalanced, i.e. $p^2 \triangleq \sum_{i=1}^{\mu} p_i^2 \neq q^2 \triangleq \sum_{i=1}^{\mu} q_i^2$. Hence, the physical model in (1) can be regarded as a generalization of the Beckmann fading model through the consideration of clustering and LoS fluctuation.

[2]or equivalently, ξ^2 is a Gamma random variable with $E[\xi^2] = 1$, shape parameter m and scale parameter $1/m$.

III. First Order Statistics

We will now provide a first-order characterization of the FB distribution in terms of its chief probability functions; as we will later see, tractable analytical expressions are attainable for its MGF, PDF and CDF. Hereinafter, we will consider the random variable $\gamma \triangleq \bar{\gamma}W/\overline{W}$, where $\overline{W} = E[W]$, representing the instantaneous SNR at the receiver side.

A. Initial Definitions

Definition 1: Let γ be a random variable characterizing the instantaneous SNR for the physical model in (1). Then, γ is said to follow a Fluctuating Beckmann (FB) distribution with mean $\bar{\gamma} = \mathbb{E}[\gamma]$ and non-negative real shape parameters κ, μ, m, η and ϱ, i.e. $\gamma \sim \mathcal{FB}(\bar{\gamma}; \kappa, \mu, m, \eta, \varrho)$, with

$$\kappa = \frac{p^2 + q^2}{\mu\left(\sigma_x^2 + \sigma_y^2\right)}, \qquad \varrho^2 = \frac{p^2}{q^2}, \qquad \eta = \frac{\sigma_x^2}{\sigma_y^2}, \tag{2}$$

μ represents the number of clusters and m accounts for the fluctuation of the LoS component.

B. First Order Statistics for the General Case

With the above definition, we now calculate the MGF of γ in the following lemma.

Lemma 1: Let $\gamma \sim \mathcal{FB}(\bar{\gamma}; \kappa, \mu, m, \eta, \varrho)$. Then, the MGF of γ is given at the top of next page in (4).

Proof: See Appendix A. ∎

Lemma 1 provides a simple closed-form expression for the MGF of the FB fading distribution. From (4), we will now show that the PDF and CDF of the FB fading distribution have a similar functional form as the κ-μ shadowed fading distribution [13].

Lemma 2: Let $\gamma \sim \mathcal{FB}(\bar{\gamma}; \kappa, \mu, m, \eta, \varrho)$. Then, the PDF of γ is given by (5) at the top of next page, where c_x and α_x, with $x = \{1, 2\}$ depend on the parameters of the FB distribution as described in the sequel, and $\Phi_2^{(n)}$ is the confluent form of the generalized Lauricella series defined in [19, eq. 7.2, pp. 446].

Proof: Manipulating (4) it is possible to write the MGF expression as follows

$$M_\gamma(s) = \frac{(-1)^\mu}{s^\mu} \frac{\alpha_2^{m-\mu/2}}{\bar{\gamma}^\mu \alpha_1^m} \left(1 - \frac{\frac{\mu(1+\eta)(1+\kappa)}{2\eta\bar{\gamma}}}{s}\right)^{m-\frac{\mu}{2}} \times \left(1 - \frac{\frac{\mu(1+\eta)(1+\kappa)}{2\bar{\gamma}}}{s}\right)^{m-\frac{\mu}{2}} \left(1 - \frac{c_1}{\bar{\gamma}s}\right)^{-m} \left(1 - \frac{c_2}{\bar{\gamma}s}\right)^{-m}, \tag{3}$$

Copyright (c) 2018 IEEE. Personal use is permitted. For any other purposes, permission must be obtained from the IEEE by emailing pubs-permissions@ieee.org.

This is the author's version of an article that has been published in this journal. Changes were made to this version by the publisher prior to publication.
The final version of record is available at http://dx.doi.org/10.1109/TVT.2017.2787204

$$M_\gamma(s) = \frac{1}{\left(1-\frac{2\eta}{\mu(1+\eta)(1+\kappa)}\bar{\gamma}s\right)^{\mu/2}\left(1-\frac{2}{\mu(1+\eta)(1+\kappa)}\bar{\gamma}s\right)^{\mu/2}} \times\left[1-\frac{1}{m}\left(\frac{\mu\kappa\left(\frac{\varrho^2}{1+\varrho^2}\right)(1+\eta)\bar{\gamma}s}{(1+\eta)(1+\kappa)\mu-2\eta\bar{\gamma}s}+\frac{\mu\kappa\left(\frac{1}{1+\varrho^2}\right)(1+\eta)\bar{\gamma}s}{(1+\eta)(1+\kappa)\mu-2\bar{\gamma}s}\right)\right]^{-m}. \quad (4)$$

$$f_\gamma(\gamma) = \frac{\alpha_2^{m-\mu/2}\gamma^{\mu-1}}{\bar{\gamma}^\mu\Gamma(\mu)\alpha_1^m}\Phi_2^{(4)}\left(-m+\frac{\mu}{2},-m+\frac{\mu}{2},m,m;\mu;\frac{-\gamma}{\bar{\gamma}\sqrt{\eta\alpha_2}},\frac{-\gamma\sqrt{\eta}}{\bar{\gamma}\sqrt{\alpha_2}},\frac{-\gamma c_1}{\bar{\gamma}},\frac{-\gamma c_2}{\bar{\gamma}}\right). \quad (5)$$

$$F_\gamma(\gamma) = \frac{\alpha_2^{m-\mu/2}\gamma^{\mu}}{\bar{\gamma}^\mu\Gamma(\mu+1)\alpha_1^m}\Phi_2^{(4)}\left(-m+\frac{\mu}{2},-m+\frac{\mu}{2},m,m;\mu+1;\frac{-\gamma}{\bar{\gamma}\sqrt{\eta\alpha_2}},\frac{-\gamma\sqrt{\eta}}{\bar{\gamma}\sqrt{\alpha_2}},\frac{-\gamma c_1}{\bar{\gamma}},\frac{-\gamma c_2}{\bar{\gamma}}\right). \quad (6)$$

where $c_{1,2}$ are the roots of $\alpha_1 s^2+\beta s+1$ with

$$\alpha_1 = \frac{4\eta}{\mu^2(1+\eta)^2(1+\kappa)^2}+\frac{2\kappa(\varrho^2+\eta)}{m(1+\varrho^2)\mu(1+\eta)(1+\kappa)^2}, \quad (7)$$

$$\beta = \frac{-1}{1+\kappa}\left[\frac{2}{\mu}+\frac{\kappa}{m}\right], \quad (8)$$

and α_2 is given by

$$\alpha_2 = \frac{4\eta}{\mu^2(1+\eta)^2(1+\kappa)^2}. \quad (9)$$

The expression for the PDF can be derived from (3) as $f_\gamma(\gamma)=\mathcal{L}^{-1}\{M_\gamma(-s)\}$ using [20, eq. 9.55], yielding (5). ■

Lemma 3: Let $\gamma\sim\mathcal{FB}(\bar{\gamma};\kappa,\mu,m,\eta,\varrho)$. Then, the CDF of γ is given by (6) at the top of this page.

Proof: Following the same steps as in the previous proof, the CDF expression is given by $F_\gamma(\gamma)=\mathcal{L}^{-1}\{\frac{M_\gamma(-s)}{s}\}$, yielding (6) directly from [20, eq. 9.55]. ■

Note that the CDF and PDF of the received signal envelope can be directly derived from (5) and (6) straightforwardly through a change of variables. Thus, we get $f_R(R)=2Rf_\gamma(R^2)$ and $F_R(R)=F_\gamma(R^2)$, with $\bar{\gamma}$ being replaced by $\Omega=E\{R^2\}$.

The PDF and CDF of the FB distribution are given in terms of the multivariate Φ_2 function, which also appears in other fading distributions in the literature [10, 13, 21]. Apparently, and because it is defined as an n-fold infinite summation, its numerical evaluation may pose some challenges from a computational point of view. However, the Laplace transform of the Φ_2 function has a comparatively simpler form in terms of a finite product of elementary functions, which becomes evident by inspecting the expression of the MGF in (4). Therefore, the Φ_2 function can be evaluated by means of a numerical inverse Laplace transform [22, 23].

As previously mentioned, the FB distribution provides the unification of a large number of important fading distributions. These connections are summarized in Table I, on which the parameters corresponding to the FB distribution are underlined in order to avoid confusion with the parameters of any of the distributions included as special cases. Notably, the Beckmann distribution arises as a special case of the more general FB distribution for $\mu=1$ and sufficiently large m. Thus, the additional degrees of freedom of the FB distribution also facilitates the anaytical characterization of the Beckmann distribution. Interestingly, when $\eta=1$ the effect of the parameter ϱ vanishes; conversely, when setting $\varrho=1$ the effect of η is still relevant. This is in coherence with the behavior of the Beckmann distribution as observed in [24].

TABLE I
CONNECTIONS BETWEEN THE FLUCTUATING BECKMANN FADING MODEL AND OTHER MODELS IN THE LITERATURE. NOTE THAT SETTING κ=0 IMPLIES THAT m AND ϱ VANISH.

Channels	Fluctuating Beckmann Fading Parameters
One-sided Gaussian	$\underline{\kappa}=0,\quad \underline{\mu}=1,\quad \underline{\eta}=0$
Rayleigh	$\underline{\kappa}=0,\quad \underline{\mu}=1,\quad \underline{\eta}=1$
Nakagami-m	$\underline{\kappa}=0,\quad \underline{\mu}=m,\quad \underline{\eta}=1$
Hoyt	$\underline{\kappa}=0,\quad \underline{\mu}=1,\quad \underline{\eta}=q$
η-μ	$\underline{\kappa}=0,\quad \underline{\mu}=\mu,\quad \underline{\eta}=\eta$
Rice	$\underline{\kappa}=K,\quad \underline{\mu}=1,\quad \underline{m}\to\infty,\quad \underline{\eta}=1\quad ,\forall\varrho$
Symmetrical η-κ	$\underline{\kappa}=\kappa,\quad \underline{\mu}=1,\quad \underline{m}\to\infty,\quad \underline{\eta}=\eta,\quad \underline{\varrho}=\eta$
Asymmetrical η-κ	$\underline{\kappa}=\kappa,\quad \underline{\mu}=1,\quad \underline{m}\to\infty,\quad \underline{\eta}=\eta,\quad \underline{\varrho}=0$
Beckmann	$\underline{\kappa}=K,\quad \underline{\mu}=1,\quad \underline{m}\to\infty,\quad \underline{\eta}=q,\quad \underline{\varrho}=r$
κ-μ	$\underline{\kappa}=\kappa,\quad \underline{\mu}=\mu,\quad \underline{m}\to\infty,\quad \underline{\eta}=1,\quad \forall\varrho$
Rician Shadowed	$\underline{\kappa}=\kappa,\quad \underline{\mu}=1,\quad \underline{m}=m,\quad \underline{\eta}=1,\quad \forall\varrho$
κ-μ shadowed	$\underline{\kappa}=\kappa,\quad \underline{\mu}=\mu,\quad \underline{m}=m,\quad \underline{\eta}=1,\quad \forall\varrho$

Under certain conditions, the PDF and CDF expressions shown in (5) and (6) can be rewritten in a much simpler way. Specifically, if the m parameter is assumed to be an integer number and the μ parameter to be an even number, (3) can be expressed in an alternative form thanks to partial fraction expansion, allowing the derivation of PDF and CDF in terms of elementary functions (i.e. exponentials and powers). This particular case is detailed in the following subsection.

C. First Order Statistics for the Special Cases

As introduced before, considering the special case in which m parameter is an integer number and μ parameter is an even

Copyright (c) 2018 IEEE. Personal use is permitted. For any other purposes, permission must be obtained from the IEEE by emailing pubs-permissions@ieee.org.

This is the author's version of an article that has been published in this journal. Changes were made to this version by the publisher prior to publication.
The final version of record is available at http://dx.doi.org/10.1109/TVT.2017.2787204

number, the PDF and the CDF of the FB fading distribution can be expressed in an alternative way which can be useful in that it simplifies further analytical purposes. Under such assumption, more tractable expressions for PDF and CDF in terms of elementary functions are calculated in the following corollaries.

Corollary 1: Let $\gamma \sim \mathcal{FB}(\bar{\gamma}; \kappa, \mu, m, \eta, \varrho)$ with m being an integer number and μ an even number. Then, the PDF of γ is given by

$$f_\gamma(\gamma) = \frac{\alpha_2^{m-\frac{\mu}{2}}}{\alpha_1^m \bar{\gamma}^\mu} \sum_{i=1}^{N(m,\mu)} e^{-\tau_i \gamma/\bar{\gamma}} \sum_{j=1}^{|\omega_i|} \frac{A_{ij}\gamma^{j-1}}{(j-1)!}, \tag{10}$$

where A_{ij} are the residues of partial fraction decomposition given by (51), constants ω_i and τ_i are the elements of vector $\boldsymbol{\omega}$ and $\boldsymbol{\tau}$, defined as

$$\boldsymbol{\omega} = \left[m, m, \frac{\mu}{2} - m, \frac{\mu}{2} - m\right], \tag{11}$$

$$\boldsymbol{\tau} = \left[c_1, c_2, \frac{\mu(1+\eta)(1+\kappa)}{2\eta}, \frac{\mu(1+\eta)(1+\kappa)}{2}\right], \tag{12}$$

and $N(m,\mu)$ is defined as

$$N(m,\mu) = 2\left[1 + \mathrm{u}\left(\frac{\mu}{2} - m\right)\right], \tag{13}$$

where $\mathrm{u}(\cdot)$ is the unit step function whose value is 1 if the argument is non-negative and 0 otherwise.

Proof: See Appendix B. ∎

Corollary 2: Let $\gamma \sim \mathcal{FB}(\bar{\gamma}; \kappa, \mu, m, \eta, \varrho)$ with m being an integer number and μ an even number. Then, the CDF of γ is given by

$$F_\gamma(\gamma) = 1 + \frac{\alpha_2^{m-\frac{\mu}{2}}}{\alpha_1^m \bar{\gamma}^\mu} \sum_{i=1}^{N(m,\mu)} e^{-\tau_i \gamma/\bar{\gamma}} \sum_{j=1}^{|\omega_i|} \frac{B_{ij}\gamma^{j-1}}{(j-1)!}. \tag{14}$$

Proof: See Appendix C. ∎

We here provide more tractable expressions for both PDF and CDF of FB distribution in terms of a finite sum of elementary functions, avoiding the use of multivariate Φ_2 function. However, this simplification comes at the price of a mild loss of generality in that both m and μ parameters are restricted to be an integer and even number, respectively.

IV. Second Order Statistics

First-order statistics such as the PDF, CDF or MGF provide valuable information about the statistical behavior of the amplitude (or equivalently power) of the received signal affected by fading. However, they do not incorporate information related to the dynamic behavior of the fading process, which is of paramount relevance in the context of wireless communications because of the relative motion of transmitter, receivers and scatterers due to mobility. In the literature, two metrics are used to capture the dynamics of a general random process: the level crossing rate (LCR), which measures how often the amplitude of the received signal crosses a given threshold value, and the average fade duration (AFD), which measures how long the amplitude of the received signal remains below this threshold [1].

A. Level Crossing Rate

The LCR of the received signal amplitude R can be computed using Rice's formula [1] as

$$N_R(u) = \int_0^\infty \dot{r} f_{R,\dot{R}}(u, \dot{r})\, d\dot{r}, \tag{15}$$

where $\dot{R}$ denotes the time derivative of the signal envelope and $f_{R,\dot{R}}(r,\dot{r})$ is the joint PDF of the received signal amplitude and its time derivative. Thus, in order to characterize the LCR of R, we must calculate the joint distribution of R and $\dot{R}$. In our derivations, we will assume that the fluctuations in the diffuse part (i.e., NLoS) occur at a smaller scale compared to those of the LoS component in the fluctuating Beckmann fading model. This is the case, for instance, on which such LoS fluctuation can be associated to shadowing.

Let us express the squared signal envelope as

$$R^2 = R_1^2 + R_2^2. \tag{16}$$

where R_1 and R_2 are defined as

$$R_1^2 = \sum_{k=1}^{\mu}(X_k + \xi p_k)^2, \quad R_2^2 = \sum_{k=1}^{\mu}(Y_k + \xi q_k)^2, \tag{17}$$

Note that both variables, when conditioned to ξ, are independent. After normalizing by $\Omega = E[R^2]$, we have that R_1 and R_2 are distributed as a κ-μ random variables, with PDF given by

$$f_{R_k}(r_k) = \frac{\Omega^{\mu/4+1/2}}{\sigma_k^2(\xi d_k)^{\mu/2-1}} r_k^{\mu/2} e^{-\frac{\Omega r_k^2}{2\sigma_k^2} - \frac{\xi^2 d_k^2}{2\sigma_k^2}} \mathrm{I}_{\mu/2-1}\left(\frac{\Omega^{1/2} r_k \xi d_k}{\sigma_k^2}\right), \tag{18}$$

where $d_1^2 = p^2 = \sum_{k=1}^{\mu} p_k^2$, $d_2^2 = q^2 = \sum_{k=1}^{\mu} q_k^2$, $\mathrm{I}_\nu(\cdot)$ is the modified Bessel function of the first kind and ξ is a Nakagami-m distributed random variable with PDF given by

$$f_\xi(\xi) = \frac{2m^m}{\Gamma(m)} \xi^{2m-1} \exp(-m\xi^2). \tag{19}$$

The derivative of R with respect to time, $\dot{R}$, can be expressed as

$$\dot{R} = \frac{\dot{R}_1 R_1 + \dot{R}_2 R_2}{R}. \tag{20}$$

Conditioned to R_1, R_2 and R, the derivative of R is a zero-mean Gaussian variable with variance

$$\sigma_{\dot{R}}^2 = \frac{\sigma_{\dot{R}_1}^2 R_1^2 + \sigma_{\dot{R}_2}^2 R_2^2}{R^2} = \frac{\sigma_{\dot{R}_1}^2 R_1^2 + \sigma_{\dot{R}_2}^2 R_2^2}{R_1^2 + R_2^2}. \tag{21}$$

Hence, the distribution of $\dot{R}$ conditioned to R_1 and R_2 is

$$f_{\dot{R}|R_1,R_2}(\dot{r}, r_1, r_2) = \frac{1}{\sqrt{2\pi\left(\frac{\sigma_{r_1}^2 r_1^2 + \sigma_{r_2}^2 r_2^2}{r_1^2 + r_2^2}\right)}} \cdot e^{-\frac{(r_1^2+r_2^2)\dot{r}^2}{2(\sigma_{r_1}^2 r_1^2 + \sigma_{r_2}^2 r_2^2)}}, \tag{22}$$

The LCR can be obtained as

$$\begin{aligned} N_R(u) &= \int_0^\infty \dot{r} f_{R,\dot{R}}(u,\dot{r}) d\dot{r} \\ &= \int_0^\infty \dot{r}\left(\int_0^u f_{\dot{R}|R,R1}(\dot{r}, u, r_1) f_{R,R1}(u, r_1) dr_1\right) d\dot{r} \\ &= \int_0^u f_{R,R_1}(u, r_1)\left(\int_0^\infty \dot{r} f_{\dot{R}|R,R_1}(\dot{r}, u, r_1) d\dot{r}\right) dr_1. \end{aligned}$$

Copyright (c) 2018 IEEE. Personal use is permitted. For any other purposes, permission must be obtained from the IEEE by emailing pubs-permissions@ieee.org.

This is the author's version of an article that has been published in this journal. Changes were made to this version by the publisher prior to publication.
The final version of record is available at http://dx.doi.org/10.1109/TVT.2017.2787204

Using the PDF of $\dot{R}$ conditioned to R and R_1 in equation (22),

$$\int_0^\infty \dot{r} f_{\dot{R}|R,R_1}(\dot{r},u,r_1)d\dot{r} = \sqrt{\frac{\sigma_{\dot{R}}^2}{2\pi}}. \tag{23}$$

The joint distribution of R_1 and R_2 can be obtained as

$$\begin{aligned} f_{R_1,R_2}(r_1,r_2) &= \int_0^\infty f_{R_1|\xi}(r_1,\xi) f_{R_2|\xi}(r_2,\xi) f_\Xi(\xi) d\xi \\ &= \frac{2m^m \Omega^{\mu/2+1}}{\Gamma(m)\sigma_1^2\sigma_2^2(pq)^{\mu/2-1}} r_1^{\mu/2} r_2^{\mu/2} \exp\left(-r_1^2\frac{\Omega}{2\sigma_1^2} - r_2^2\frac{\Omega}{2\sigma_2^2}\right) \times \\ &\int_0^\infty \left\{ \xi^{2m-\mu+1} \exp\left(-\xi^2\left(\frac{p^2}{2\sigma_1^2}+\frac{q^2}{2\sigma_2^2}+m\right)\right) \times \right. \\ &\left. \mathrm{I}_{\mu/2-1}\left(\frac{\Omega^{1/2} r_1 \xi p}{\sigma_1^2}\right) \mathrm{I}_{\mu/2-1}\left(\frac{\Omega^{1/2} r_2 \xi q}{\sigma_2^2}\right) d\xi \right\}. \end{aligned} \tag{24}$$

In the general case, the last integral cannot be solved analytically in closed-form, to the best of the authors' knowledge.

B. Level Crossing Rate for Independent In-Phase and Quadrature Components

As can be seen, the LCR obtained in the previous section involves the calculation of two integrals. It is possible to arrive at a more tractable expression for a simpler yet general case by considering the scenario in which in-phase and quadrature components are independent. We note, however, that such a scenario is still a FB fading model, and does not bear any similarity with any other previous model published in the literature. Independence between in-phase and quadrature components can be achieved by assuming $q_i = 0$ and $p_i \neq 0$ or vice-versa in (1).

Assuming the special case of $q_i = 0$ (the case of $p_i = 0$ can be solved similarly) in which R_1 and R_2 are independent, the distribution of $f_{R,R_1}(r,r_1)$ can be obtained as

$$\begin{aligned} f_{R,R_1}(u,r_1) &= |J_{r_1,r_2}(u,r_1)| f_{R_1,R_2}(r_1,\sqrt{u^2-r_1^2}) \\ &= |J_{r_1,r_2}(u,r_1)| f_{R_1}(r_1) f_{R_2}(\sqrt{u^2-r_1^2}) \\ &= \frac{m^m \Omega^\mu u \cdot r_1^{\mu-1} \cdot (u^2-r_1^2)^{\mu/2-1}}{2^{\mu-2}\Gamma^2(\mu/2)\sigma_1^\mu\sigma_2^\mu(\frac{p^2}{2\sigma_1^2}+m)^m} \times \\ &\quad e^{-\frac{\Omega(u^2-r_1^2)}{2\sigma_2^2} - \frac{\Omega r_1^2}{2\sigma_1^2}} \cdot {}_1F_1\left(m,\mu/2;\frac{\Omega\frac{p^2}{4\sigma_1^4}}{\frac{p^2}{2\sigma_1^2}+m} r_1^2\right), \end{aligned} \tag{25}$$

for $0 \leq r_1 \leq r$, where $|J_{r_1,r_2}(\cdot,\cdot)|$ denotes the Jacobian of the transformation of random variables and ${}_1F_1(\cdot)$ is the confluent hypergeometric function [25]. In this particular case, the LCR of the normalized envelope R can be expressed as

$$\begin{aligned} N_R(u) &= \frac{m^m \Omega^\mu u}{2^{\mu-2}\Gamma^2(\mu/2)\sigma_1^\mu\sigma_2^\mu(\frac{p^2}{2\sigma_1^2}+m)^m\sqrt{2\pi}} \times \\ &\int_0^u \left(\sigma_{\dot{R}_1}^2 r_1^2/u^2 + \sigma_{\dot{R}_2}^2(1-r_1^2/u^2)\right)^{\frac{1}{2}} (u^2-r_1^2)^{\mu/2-1} \times \\ &r_1^{\mu-1} e^{-\frac{\Omega(u^2-r_1^2)}{2\sigma_2^2} - \frac{\Omega r_1^2}{2\sigma_1^2}} {}_1F_1\left(m,\tfrac{\mu}{2};\frac{\Omega\frac{p^2}{4\sigma_1^4}}{\frac{p^2}{2\sigma_1^2}+m} r_1^2\right) dr_1, \end{aligned} \tag{26}$$

and after a change of variables we have

$$\begin{aligned} N_R(u) &= \frac{m^m \Omega^\mu u^{(2\mu-1)}}{2^{\mu-1}\Gamma^2(\mu/2)\sigma_1^\mu\sigma_2^\mu(\frac{p^2}{2\sigma_1^2}+m)^m\sqrt{2\pi}} \cdot e^{-\frac{\Omega u^2}{2\sigma_2^2}} \times \\ &\int_0^1 [\sigma_{\dot{R}_2}^2 + (\sigma_{\dot{R}_1}^2 - \sigma_{\dot{R}_2}^2)x]^{\frac{1}{2}} (1-x)^{(\mu/2-1)} x^{(\mu/2-1)} \times \\ &e^{-\frac{\Omega(\sigma_2^2-\sigma_1^2)u^2 x}{2\sigma_1^2\sigma_2^2}} {}_1F_1\left(m,\tfrac{\mu}{2};\frac{\Omega\frac{p^2}{4\sigma_1^4}}{\frac{p^2}{2\sigma_1^2}+m} u^2 x\right) dx, \end{aligned} \tag{27}$$

where $\sigma_{\dot{R}_1}^2 = \frac{-\ddot{\rho}(0)\sigma_1^2}{\Omega}$ and $\sigma_{\dot{R}_2}^2 = \frac{-\ddot{\rho}(0)\sigma_2^2}{\Omega}$ from (21), and $\ddot{\rho}(0)$ is the second derivative of the autocorrelation function evaluated at 0.

Finally, (26) can be expressed in terms of the parameters of the FB distribution[3], yielding

$$\begin{aligned} N_R(u) &= \frac{m^m[\mu(1+\eta)(1+\kappa)]^{\mu-1/2}\sqrt{-\ddot{\rho}(0)}}{2^{\mu-1}\Gamma^2(\mu/2)\eta^{\mu/2}(\frac{\mu\kappa(1+\eta)}{2\eta}+m)^m\sqrt{2\pi}} \cdot u^{(2\mu-1)} \times \\ &e^{-\mu/2(1+\eta)(1+\kappa)u^2} \int_0^1 [1+(\eta-1)x]^{\frac{1}{2}} (1-x)^{(\mu/2-1)} x^{(\mu/2-1)} \times \\ &e^{-\frac{\mu(1-\eta^2)(1+\kappa)}{2\eta}u^2 x} {}_1F_1\left(m,\mu/2;\frac{\frac{\kappa\mu^2(1+\eta)^2(1+\kappa)}{4\eta^2}}{\frac{\mu\kappa(1+\eta)}{2\eta}+m} u^2 x\right) dx. \end{aligned} \tag{28}$$

Note that, although above result for the LCR has been derived for the special case $q_i = 0$, it is fully equivalent to the case with $p_i = 0$ just setting $\eta \to 1/\eta$, since both cases are actually the same, as can be seen in (1).

C. Average Fade Duration

With the knowledge of the LCR and the CDF of the FB distribution, the AFD can be directly obtained as

$$T_R(u) = \frac{F_R(u)}{N_R(u)}, \tag{29}$$

where $F_R(u)$ is the CDF of the fading amplitude envelope derived in (6), after a proper change of variables.

V. Numerical Results and Applications

A. First Order Statistics

After attaining a full statistical characterization of the newly proposed Fluctuating Beckmann fading distribution, we aim to exemplify the influence of the parameters of this fading model over the distribution of the received amplitude. We will first focus on understanding the effect of the power imbalance in the LoS and NLoS components (i.e. the effect of ϱ and η), since these are the two parameters that effectively extend the original κ-μ shadowed fading model to a more general case. Monte Carlo simulations are provided in order to double-check the validity of the derived expressions.

In Figs. 1 and 2, the PDF of the received signal amplitude is represented for different values of NLoS power imbalance

[3]Note that, because of the assumption of $q_k = 0$, this implies that the parameter $\varrho \to \infty$.

Copyright (c) 2018 IEEE. Personal use is permitted. For any other purposes, permission must be obtained from the IEEE by emailing pubs-permissions@ieee.org.

This is the author's version of an article that has been published in this journal. Changes were made to this version by the publisher prior to publication.
The final version of record is available at http://dx.doi.org/10.1109/TVT.2017.2787204

η and LoS fluctuation severity m. The values $m = 1$ and $m = 10$ correspond to the cases of heavy and mild fluctuation of the LoS component, respectively. The parameter ϱ is set to $\varrho^2 = 0.1$, indicating a moderately large LoS power imbalance, and $\mu = 1$. Let us first focus on Fig. 1, where we set $\kappa = 1$ to indicate a weak LoS scenario on which the LoS and NLoS power is the same. We observe that the effect of increasing η causes the amplitude values to be more concentrated around its mean value. Besides, compared to the case of $\eta = 1$ (i.e. the κ-μ shadowed fading distribution), the effect of having a power imbalance in the NLoS component clearly has an impact on the distribution of the signal envelope. Differently from the η-μ fading model, the behavior of the distribution with respect to η is no longer symmetrical between $\eta \in [0, 1]$ and $\eta \in [1, \infty)$ for a fixed $\varrho \neq 1$. One interesting effect comes from the observation of the effect of increasing η: both setting $\eta = 0.1$ or $\eta = 10$ implies that the NLoS power is imbalanced by a factor of 10. However, it is evident that if this NLoS imbalance goes to the component associated with a larger LoS imbalance ($\eta = 0.1$ since we have $\varrho^2 = 0.1$), this is way more detrimental for the received signal envelope than having the NLoS imbalance in the other component.

Fig. 2 now considers a strong LoS scenario on which $\kappa = 10$. The rest of the parameters are the same ones as in the previous figure. Because the LoS component is now much more relevant, the effect of changing m is more noticeable. We observe that for $m = 10$, which corresponds to a mild fluctuation on the LoS component, the shape of the PDF is only slightly altered when changing η. Conversely, the shape of the PDF is more affected by η for low values of amplitude when $m = 1$. This is further exemplified in Fig. 3, on which a bimodal behavior is observed as the imbalance is reduced through ϱ or η. When both $\{\varrho, \eta\}$ decrease, the in-phase components have considerably less power than the quadrature components. Because κ is sufficiently large, the distribution will mostly fluctuate close to the LoS part of the quadrature component due to m, and the first maximum on the PDF in the low-amplitude region appears as the highly imbalanced in-phase component only is able to contribute in this region. We must note that this bimodal behavior does not appear in the original κ-μ shadowed or Beckmann distributions from which the FB distribution originates. Nevertheless, such bimodality indeed shows in other fading models such as the α-η-κ-μ [8], the two-wave with diffuse power [26], the fluctuating two-ray [21] and some others [18, 27].

We represent in Figs. 4 and 5 the PDF of the received signal amplitude for different values of LoS power imbalance ϱ and LoS fluctuation severity m. We first consider the weak LoS scenario with $\kappa = 1$, and setting $\mu = 2$ and $\eta = 0.1$. We observe that low values of ϱ and m cause the amplitude values being more sparse. When the LoS component is stronger, i.e. $\kappa = 10$ in Fig. 5 the effect of increasing m (i.e. eliminating the LoS fluctuation) or ϱ is more relevant.

Figs. 6 and 7 are useful to understanding the effect of the parameters ϱ and η over the CDF. Spefically, in Fig. 6 we compare the shape of the CDF in weak and strong LoS scenarios as η varies. The LoS fluctuation parameter is set to $m = 10$ in order to eliminate its influence, whereas $\varrho^2 = 0.1$ and $\mu = 1$. We observe that increasing either η or κ makes the slope of the CDF rise close to $x = 1$. A similar observation can be made when inspecting Fig. 7. We see that having the LoS and NLoS imbalances in the same component ($\varrho^2 = \eta = 0.1$) is more detrimental for the signal envelope, and the probability of having very low values of signal level is higher.

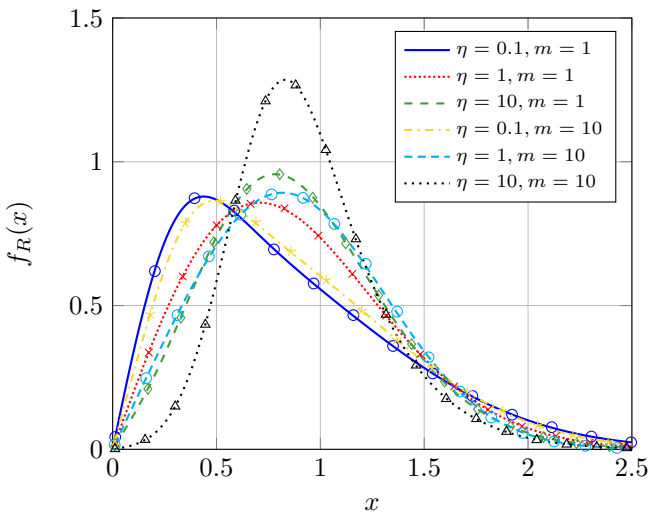

Fig. 1. FB signal envelope distribution for different values of η and m in weak LoS scenario ($\kappa = 1$) with $\varrho^2 = 0.1$, $\mu = 1$ and $\Omega = E\{R^2\} = 1$. Solid lines correspond to the exact PDF, markers correspond Monte Carlo simulations.

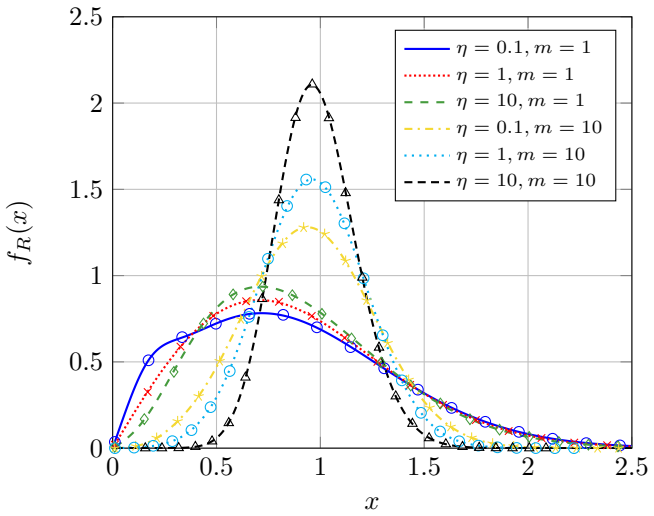

Fig. 2. FB signal envelope distribution for different values of η and m in strong LoS scenario ($\kappa = 10$) with $\varrho^2 = 0.1$, $\mu = 1$ and $\Omega = E\{R^2\} = 1$. Solid lines correspond to the exact PDF, markers correspond Monte Carlo simulations.

B. Second Order Statistics

We will now investigate the effect of the FB fading parameters on the second-order statistics of the distribution. We assume that a time variation of the diffuse component according to Clarke's correlation model [28] with maximum Doppler shift f_d; this implies that $\sqrt{-\ddot{\rho}} = \sqrt{2} f_d \pi$ [29]. As argued in Section IV, we consider that $\varrho \to \infty$ and

Copyright (c) 2018 IEEE. Personal use is permitted. For any other purposes, permission must be obtained from the IEEE by emailing pubs-permissions@ieee.org.

This is the author's version of an article that has been published in this journal. Changes were made to this version by the publisher prior to publication.
The final version of record is available at http://dx.doi.org/10.1109/TVT.2017.2787204

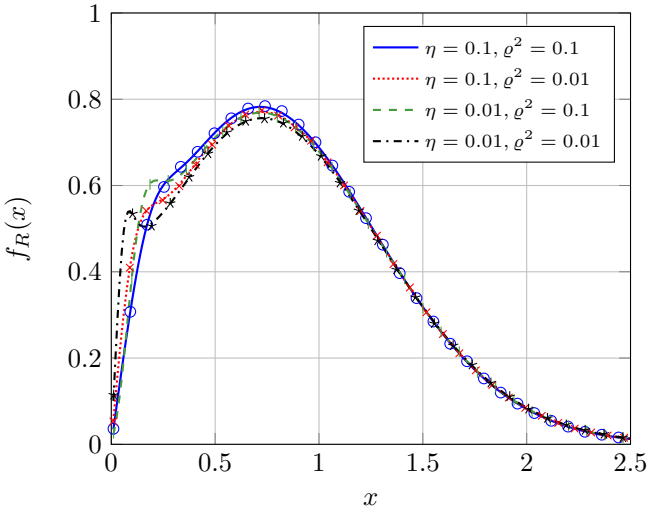

Fig. 3. FB signal envelope distribution for different values of η and ϱ in strong LoS scenario ($\kappa = 10$) with $m = 1$, $\mu = 1$ and $\Omega = E\{R^2\} = 1$. Solid lines correspond to the exact PDF, markers correspond Monte Carlo simulations.

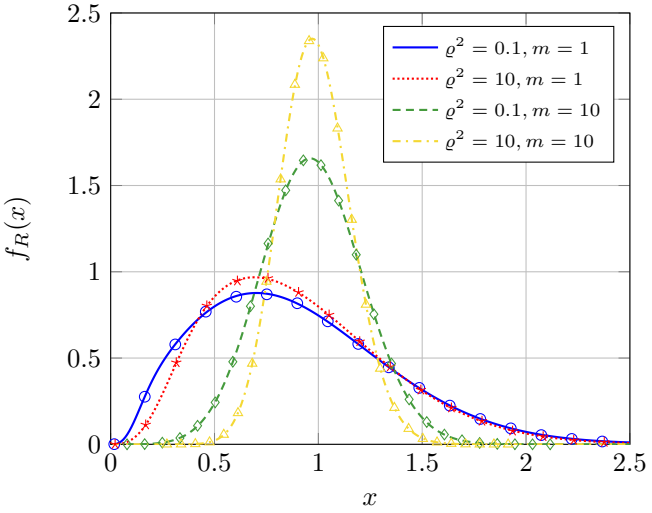

Fig. 5. FB signal envelope distribution for different values of ϱ and m in strong LoS scenario($\kappa = 10$) with $\eta = 0.1$, $\mu = 2$ and $\Omega = E\{R^2\} = 1$. Solid lines correspond to the exact PDF, markers correspond Monte Carlo simulations.

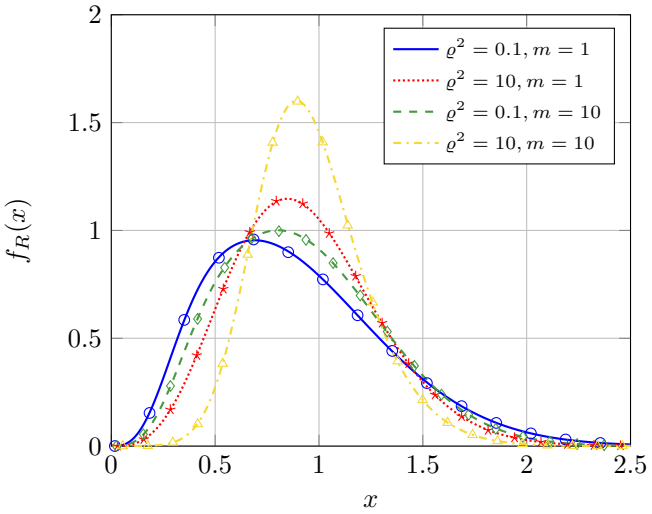

Fig. 4. FB signal envelope distribution for different values of ϱ and m in weak LoS scenario ($\kappa = 1$) with $\eta = 0.1$, $\mu = 2$ and $\Omega = E\{R^2\} = 1$. Solid lines correspond to the exact PDF derived, markers correspond Monte Carlo simulations.

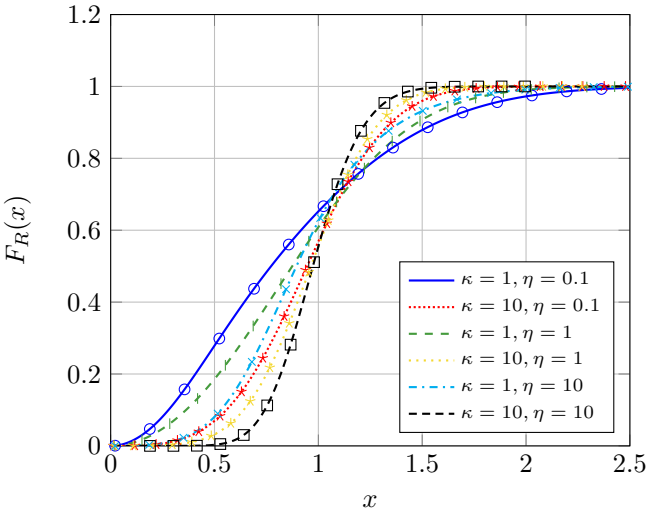

Fig. 6. FB signal envelope CDF for different values of κ and η with $\varrho^2 = 0.1$, $\mu = 1$, $m = 10$ and $\Omega = E\{R^2\} = 1$. Solid lines correspond to the exact CDF, markers correspond Monte Carlo simulations.

hence the LCR and AFD are given by (28) and (29). Monte Carlo simulations are also included, by generating a sampled fluctuating Beckmann random process with sampling period $T_s >> f_d$ in order to avoid missing level crossings at very low threshold values [30].

Fig. 8 represents the LCR vs the normalized threshold for different sets of fading parameter values. When increasing μ, i.e. the number of multipath clusters, the number of crossings at very low threshold values is drastically reduced. Similarly, the number of crossings in this region grows when reducing κ or increasing η. This latter effect is coherent with the fact that $\varrho \to \infty$ in this case, so that having a value of $\eta < 1$ is beneficial in terms of fading severity. Thus, the maximum number of crossings for low threshold values in the investigated scenarios is attained for low μ and κ, and large η.

Fig. 9 represents the AFD vs the normalized threshold for the same set of fading parameter values as in Fig. 8. Interestingly, we see that the duration of deep fades is not affected by η. We also observe that a larger AFD is associated with a lower value of μ and a larger value of κ; this is in coherence with the observations in [31] for the particular case of the κ-μ fading model.

C. Error Probability Analysis

We now exemplify how the performance analysis of wireless communication systems operating under FB fading can be carried out. For the sake of simplicity, we here focus on the

Copyright (c) 2018 IEEE. Personal use is permitted. For any other purposes, permission must be obtained from the IEEE by emailing pubs-permissions@ieee.org.

This is the author's version of an article that has been published in this journal. Changes were made to this version by the publisher prior to publication.
The final version of record is available at http://dx.doi.org/10.1109/TVT.2017.2787204

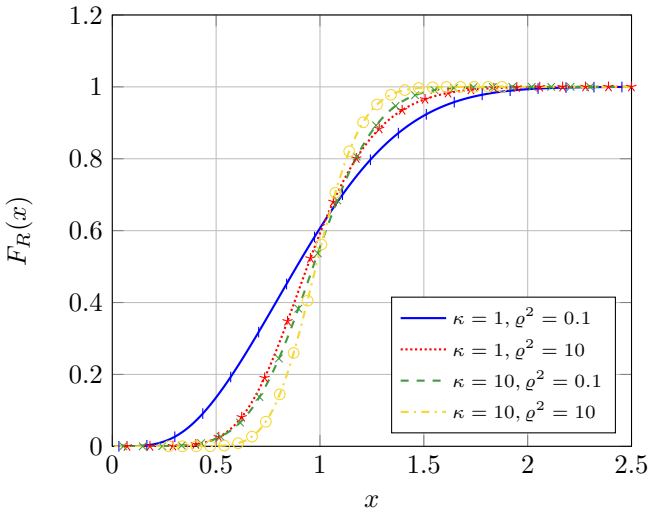

Fig. 7. FB signal envelope CDF for different values of κ and ϱ with $\eta = 0.1$, $\mu = 2$, $m = 10$ and $\Omega = E\{R^2\} = 1$. Solid lines correspond to the exact CDF, markers correspond Monte Carlo simulations.

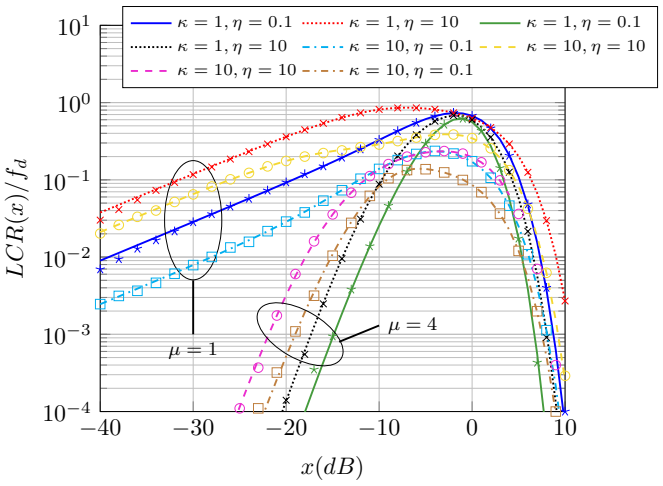

Fig. 8. Normalized LCR vs threshold value x (dB) normalized to Ω for different values of κ, η and μ, with $m = 1$ and $\varrho \to \infty$. Solid lines correspond to the exact LCR, markers correspond Monte Carlo simulations.

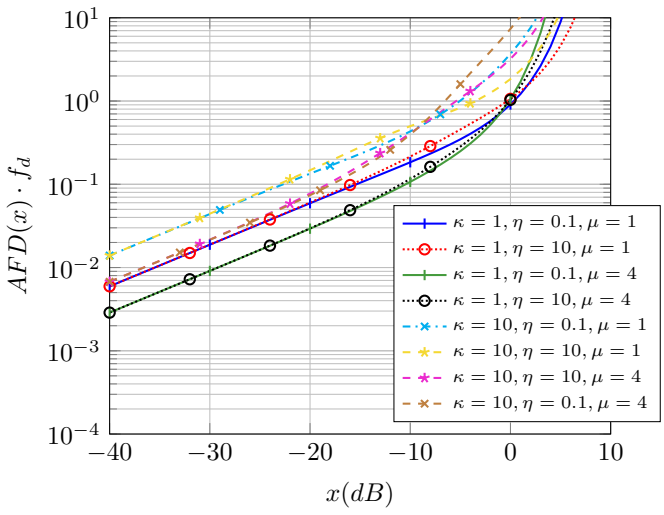

Fig. 9. Normalized AFD vs threshold value x (dB) normalized to Ω for different values of κ, η and μ, with $m = 1$ and $\varrho \to \infty$. Solid lines correspond to the exact AFD, markers correspond Monte Carlo simulations.

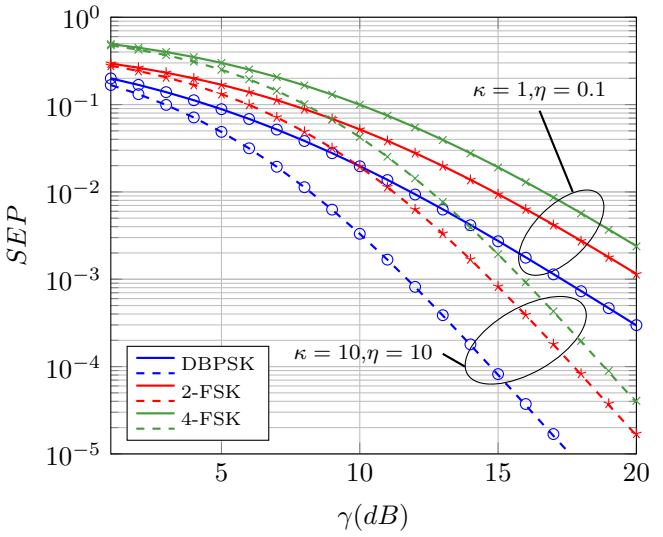

Fig. 10. SEP vs. γ for different values of κ and η and different modulation schemes. Parameter values are $m = 4$, $\mu = 2$ and $\varrho^2 = 0.2$. Solid lines correspond to the exact SEP, markers correspond Monte Carlo simulations.

symbol error probability (SEP) analysis for a number of well-known modulation schemes.

The SEP in the presence of fading is known to be given by

$$P_s(\bar{\gamma}) = \int_0^\infty P_{AWGN}(\gamma) f_\gamma(\gamma) d\gamma, \tag{30}$$

where $P_{AWGN}(\gamma)$ is the symbol error probability in the AWGN case, which is given by [5, eq. 8.85] when using coherent DBPSK (Differential Binary Phase-Shift Keying) modulation. Since the SEP of DBPSK modulation has exponential form, introducing this in the above equation yields

$$P_s(\bar{\gamma}) = \frac{1}{2} \int_0^\infty e^{-\gamma} f_\gamma(\gamma) d\gamma, \tag{31}$$

which is fully equivalent to

$$P_s(\bar{\gamma}) = \frac{1}{2} M_\gamma(s)|_{s=-1}. \tag{32}$$

Thus, the SEP of DPBSK when assuming the FB fading model is given in (34) at the top of next page.

In the case of assuming orthogonal M-ary FSK (Frequency-Shift Keying) signals and non-coherent demodulation, the symbol error probability over AWGN channels is given in [5, eq. 8.67] as

$$P_s(\bar{\gamma}) = \sum_{n=1}^{M-1} (-1)^{n+1} \binom{M-1}{n} \frac{1}{n+1} M_\gamma(s)\Big|_{s=\frac{-n}{n+1}}, \tag{33}$$

yielding the expression given in (35) at the top of next page when assuming the FB fading model.

The SEP is evaluated in Fig. 10, assuming coherent DBPSK, and non-coherent 2-FSK and 4-FSK. We observe that the SEP performance of DBPSK is much better than the non-coherent

Copyright (c) 2018 IEEE. Personal use is permitted. For any other purposes, permission must be obtained from the IEEE by emailing pubs-permissions@ieee.org.

This is the author's version of an article that has been published in this journal. Changes were made to this version by the publisher prior to publication.
The final version of record is available at http://dx.doi.org/10.1109/TVT.2017.2787204

$$P_s(\bar{\gamma}) = \frac{1}{2\left(1+\frac{2\eta}{\mu(1+\eta)(1+\kappa)}\bar{\gamma}\right)^{\mu/2}\left(1+\frac{2}{\mu(1+\eta)(1+\kappa)}\bar{\gamma}\right)^{\mu/2}} \times \left[1+\frac{1}{m}\left(\frac{\mu\kappa\left(\frac{\varrho^2}{1+\varrho^2}\right)(1+\eta)\bar{\gamma}}{(1+\eta)(1+\kappa)\mu+2\eta\bar{\gamma}} + \frac{\mu\kappa\left(\frac{1}{1+\varrho^2}\right)(1+\eta)\bar{\gamma}}{(1+\eta)(1+\kappa)\mu+2\bar{\gamma}}\right)\right]^{-m}. \quad (34)$$

$$P_s(\bar{\gamma}) = \sum_{n=1}^{M-1}(-1)^{n+1}\binom{M-1}{n}\frac{1}{n+1} \times \frac{1}{\left(1+\frac{2n\eta}{(n+1)\mu(1+\eta)(1+\kappa)}\bar{\gamma}\right)^{\mu/2}} \times \frac{1}{\left(1+\frac{2n}{(n+1)\mu(1+\eta)(1+\kappa)}\bar{\gamma}\right)^{\mu/2}} \times \left[1+\frac{1}{m}\left(\frac{\mu\kappa\left(\frac{\varrho^2}{1+\varrho^2}\right)(1+\eta)\bar{\gamma}\left(\frac{n}{n+1}\right)}{(1+\eta)(1+\kappa)\mu+2\eta\bar{\gamma}\left(\frac{n}{n+1}\right)} + \frac{\mu\kappa\left(\frac{1}{1+\varrho^2}\right)(1+\eta)\bar{\gamma}\left(\frac{n}{n+1}\right)}{(1+\eta)(1+\kappa)\mu+2\bar{\gamma}\left(\frac{n}{n+1}\right)}\right)\right]^{-m}. \quad (35)$$

schemes, especially when the fading severity is reduced (i.e. large κ and η, for $\varrho < 1$)

VI. Conclusion

We presented an extension of the κ-μ shadowed fading distribution, by including the effects of power imbalance between the LoS and NLoS components through two additional parameters, ϱ and η, respectively. This generalization also includes the classical and notoriously unwieldy Beckmann fading distribution as special case, with the advantage of admitting a relatively simple analytical characterization when compared to state-of-the-art fading models. Thus, we are able to unify a wide set of fading models in the literature under the umbrella of a more general model, for which we suggest the name of Fluctuating Beckmann fading model.

We observed that when the LoS and NLoS imbalances are both large for the same component (i.e. $\varrho < 1$ and $\eta < 1$ for the in-phase component, or $\varrho > 1$ and $\eta > 1$ for the quadrature component), the fading severity is increased. Conversely, when the LoS imbalance is larger in one component (e.g. $\varrho < 1$) it is beneficial that its NLoS part has less power (i.e. $\eta > 1$ in this case) in order to reduce fading severity. Strikingly and somehow counterintuitively, the FB distribution exhibits a bimodal behavior in some specific scenarios, unlike the distributions from which it originates.

Appendix A
Proof of Lemma I

Let us consider the physical model in (1). Specializing for $\mu = 1$, the conditional MGF of the signal power W given ξ follows a Beckmann distribution with MGF given by [5, eq. 2.38]

$$M_W(s|\xi) = \frac{1}{(1-2\sigma_x^2 s)^{1/2}(1-2\sigma_y^2 s)^{1/2}} \times \exp\left(\frac{p_1^2\xi s}{1-2\sigma_x^2 s} + \frac{q_1^2\xi s}{1-2\sigma_y^2 s}\right). \quad (36)$$

Since the Gaussian processes within (1) are mutually independent, then the conditional moment-generating function of the FB distribution can be obtained by multiplying the μ terms of the sum. Thus, the conditional MGF of the signal power W is given by

$$M_W(s|\xi) = \frac{1}{(1-2\sigma_x^2 s)^{\mu/2}(1-2\sigma_y^2 s)^{\mu/2}} \times \exp\left(\frac{p^2\xi s}{1-2\sigma_x^2 s} + \frac{q^2\xi s}{1-2\sigma_y^2 s}\right), \quad (37)$$

where $p^2 = \sum_{i=1}^{\mu} p_i^2$ and $q^2 = \sum_{i=1}^{\mu} q_i^2$.

With the definitions in (2), the conditional MGF in (37) can be rewritten as:

$$M_\gamma(s|\xi) = \frac{1}{\left(1-\frac{2\eta}{\mu(1+\eta)(1+\kappa)}\bar{\gamma}s\right)^{\mu/2}\left(1-\frac{2}{\mu(1+\eta)(1+\kappa)}\bar{\gamma}s\right)^{\mu/2}} \times exp\left(\frac{\mu\kappa\left(\frac{\varrho^2}{1+\varrho^2}\right)(1+\eta)\xi\bar{\gamma}s}{(1+\eta)(1+\kappa)\mu-2\eta\bar{\gamma}s} + \frac{\mu\kappa\left(\frac{1}{1+\varrho^2}\right)(1+\eta)\xi\bar{\gamma}s}{(1+\eta)(1+\kappa)\mu-2\bar{\gamma}s}\right). \quad (38)$$

Finally, the unconditional MGF for the FB fading model can be obtained by averaging (38) as

$$M_\gamma(s) = \int_0^\infty M_\gamma(s|\xi)\, f_\xi(\xi)\, d\xi, \quad (39)$$

where $f_\xi(\xi)$ is the Nakagami-m PDF, yielding (4).

Appendix B
Proof of Corollary I

The expression for the PDF can be derived as $f_\gamma(\gamma) = \mathcal{L}^{-1}\{M_\gamma(-s)\}$ as in the general case. Manipulating (3) and evaluating it at $s = -s$ it is possible to write

$$M_\gamma(-s) = \frac{\alpha_2^{m-\frac{\mu}{2}}}{\alpha_1^m\bar{\gamma}^\mu}\left(s+\frac{\mu(1+\eta)(1+\kappa)}{2\eta\bar{\gamma}}\right)^{m-\frac{\mu}{2}} \times \left(s+\frac{\mu(1+\eta)(1+\kappa)}{2\bar{\gamma}}\right)^{m-\frac{\mu}{2}}\left(s+\frac{c_1}{\bar{\gamma}}\right)^{-m}\left(s+\frac{c_2}{\bar{\gamma}}\right)^{-m}, \quad (40)$$

where, taking partial fraction expansion the expression for $M_\gamma(-s)$ yields

$$M_\gamma(-s) = \frac{\alpha_2^{m-\frac{\mu}{2}}}{\alpha_1^m\bar{\gamma}^\mu}\sum_{i=1}^{N(m,\mu)}\sum_{j=1}^{|\omega_i|}\frac{A_{ij}}{(s+\tau_i/\bar{\gamma})^j}, \quad (41)$$

Copyright (c) 2018 IEEE. Personal use is permitted. For any other purposes, permission must be obtained from the IEEE by emailing pubs-permissions@ieee.org.

This is the author's version of an article that has been published in this journal. Changes were made to this version by the publisher prior to publication.
The final version of record is available at http://dx.doi.org/10.1109/TVT.2017.2787204

with ω_i and τ_i the elements of vectors $\boldsymbol{\omega}$ and $\boldsymbol{\tau}$ given by (11) and (12), N a constant defined in (13) and $A_{i,j}$ the partial fraction decomposition residues given by (51), whose calculation is detailed in D.

Thanks to this new expression for the MGF, the PDF can be obtained directly using the Laplace transform pair [32]

$$\mathcal{L}^{-1}\left\{\frac{1}{(s+\nu)^n}\right\} = \frac{t^{n-1}}{(n-1)!}e^{-\nu t}, \tag{42}$$

yielding the expression for the PDF shown in (10).

Appendix C
Proof of Corollary II

Proceeding analogously to the PDF case, the CDF expression is given by $F_\gamma(\gamma) = \mathcal{L}^{-1}\left\{\frac{M_\gamma(-s)}{s}\right\}$. From MGF expression shown in (3), it is possible to write

$$\frac{M_\gamma(-s)}{s} = \frac{\alpha_2^{m-\frac{\mu}{2}}}{\alpha_1^m \bar{\gamma}^\mu}\frac{1}{s}\left(s+\tfrac{\mu(1+\eta)(1+\kappa)}{2\eta\bar{\gamma}}\right)^{m-\frac{\mu}{2}} \times \left(s+\tfrac{\mu(1+\eta)(1+\kappa)}{2\bar{\gamma}}\right)^{m-\frac{\mu}{2}}\left(s+\tfrac{c_1}{\bar{\gamma}}\right)^{-m}\left(s+\tfrac{c_2}{\bar{\gamma}}\right)^{-m}, \tag{43}$$

where partial expansion leads us to

$$\frac{M_\gamma(-s)}{s} = \frac{\alpha_2^{m-\frac{\mu}{2}}}{\alpha_1^m \bar{\gamma}^\mu}\left(\frac{B_s}{s} + \sum_{i=1}^{N(m,\mu)}\sum_{j=1}^{|\omega_i|}\frac{A_{ij}}{(s+\tau_i/\bar{\gamma})^j}\right), \tag{44}$$

where constants ω_i, τ_i and N are the same as in PDF case, which are defined in (11), (12) and (13), respectively. As before, B_s and $B_{i,j}$ are the partial fraction decomposition residues given by (50) and (52), whose derivation is detailed in Appendix D. Applying the Laplace transform pair listed in (42), and after some algebraic manipulations, we arrive to the CDF expression given in (14).

Appendix D
Derivation of Partial Fraction Expansion Residues

The general expression for partial expansion residues is given in [32, eq. A.36], which allows us to write A_{ij} and B_{ij} as

$$A_{ij} = \frac{1}{(|\omega_i|-j)!}\frac{d^{|\omega_i|-j}}{ds^{|\omega_i|-j}}\left[\prod_{\substack{k=1\\k\neq i}}^{4}\left(s+\tfrac{\tau_k}{\bar{\gamma}}\right)^{-\omega_k}\right]\Bigg|_{s=\frac{-\tau_i}{\bar{\gamma}}}, \tag{45}$$

$$B_{ij} = \frac{1}{(|\omega_i|-j)!}\frac{d^{|\omega_i|-j}}{ds^{|\omega_i|-j}}\left[\frac{1}{s}\prod_{\substack{k=1\\k\neq i}}^{4}\left(s+\tfrac{\tau_k}{\bar{\gamma}}\right)^{-\omega_k}\right]\Bigg|_{s=\frac{-\tau_i}{\bar{\gamma}}}, \tag{46}$$

where each one is obtained as a $|\omega_i|-j$-th order derivative, which can be tedious of computing. In the following, a closed-form expression for the residues is presented.

Focusing on A_{ij} residues, (45) can be rewritten using the general Leibniz rule, which gives

$$A_{ij} = \frac{1}{(|\omega_i|-j)!}\left(\sum_{k_1+\ldots k_3=|\omega_i|-j}\binom{|\omega_i|-j}{k_1\ldots k_3}\times \prod_{\substack{z=1\\z\neq i}}^{4}\left[\left(s+\tau_z/\bar{\gamma}\right)^{-\omega_z}\right]^{(k_z)}\right)\Bigg|_{s=-\tau_i/\bar{\gamma}}, \tag{47}$$

where $\binom{|\omega_i|-j}{k_1\ldots k_3} = \frac{(|\omega_i|-j)!}{k_1!k_2!k_3!}$. The sum condition $k_1+\ldots k_3 = |\omega_i|-j$ represents that there are as many terms as combinations of k_1, k_2 and k_3 exist that fulfil $\sum_{t=1}^{3} k_t = |\omega_i|-j$.

General Leibniz rule has allowed us to express derivatives of the rational polynomial as the product of the binomials derivatives. Moreover, closed-form expressions for binomial derivatives are given below

$$\frac{d^q}{ds^q}(s+\alpha)^\nu = \begin{cases}\frac{(\nu)!}{(\nu-q)!}(s+\alpha)^{\nu-q} & \text{if } \nu \geq 0\\ (-1)^q(-\nu)_q(s+\alpha)^{\nu-q} & \text{if } \nu < 0\end{cases}. \tag{48}$$

We see that the number of poles the MGF (and consequently the closed-form expression for each binomial derivative) is a function of m and μ parameters. Thus, it is necessary to distinguish between the cases where $m \geq \mu/2$, and $m < \mu/2$, respectively. Taking this into consideration, and introducing the above equation in (47), the final expression for the residues A_{ij} is given in (51) at the top of the next page.

Following the same steps as with A_{ij} residues, the final result for B_{ij} constants after applying the general Leibniz rule and introducing the closed-form derivatives expressions is also shown in (52) at the top of the next page, where the same cases has been considered.

Finally, the residue B_s is given by

$$B_s = \left(\prod_{k=1}^{4}\left(s+\tau_k/\bar{\gamma}\right)^{-\omega_k}\right)\Bigg|_{s=0}, \tag{49}$$

which immediately leads to

$$B_s = \prod_{k=1}^{4}\left(\tau_k/\bar{\gamma}\right)^{-\omega_k}. \tag{50}$$

References

[1] S. O. Rice, "Mathematical analysis of random noise," *The Bell System Technical Journal*, vol. 23, no. 3, pp. 282–332, July 1944.
[2] R. S. Hoyt, "Probability functions for the modulus and angle of the normal complex variate," *Bell System Technical Journal*, vol. 26, no. 4, pp. 318–359, Apr. 1947.
[3] P. Beckmann, "Statistical distribution of the amplitude and phase of a multiply scattered field," *JOURNAL OF RESEARCH of the National Bureau of Standards-D. Radio Propagation*, vol. 66D, no. 3, pp. 231–240, 1962.
[4] ——, "Rayleigh distribution and its generalizations," *RADIO SCIENCE Journal of Research NBS/USNC-URSI*, vol. 68D, no. 9, pp. 927–932, September 1964.
[5] M. K. Simon and M.-S. Alouini, *Digital communication over fading channels*. Wiley-IEEE Press, 2005. [Online]. Available: http://www.worldcat.org/isbn/0471649538

Copyright (c) 2018 IEEE. Personal use is permitted. For any other purposes, permission must be obtained from the IEEE by emailing pubs-permissions@ieee.org.

This is the author's version of an article that has been published in this journal. Changes were made to this version by the publisher prior to publication.
The final version of record is available at http://dx.doi.org/10.1109/TVT.2017.2787204

$$A_{ij} = \begin{cases} \sum\limits_{\substack{k_1+\ldots k_3=m-j \\ k_1,k_2\leq m-\mu/2}} \left[\frac{1}{\prod_{t=1}^{3} k_t!} \prod\limits_{l=1}^{2} \frac{(m-\frac{\mu}{2})!}{(m-\frac{\mu}{2}-k_l)!} \left(\frac{\tau_l}{\bar{\gamma}} - \frac{\tau_i}{\bar{\gamma}}\right)^{m-\frac{\mu}{2}-k_l} \prod\limits_{\substack{z=3 \\ z\neq i}}^{4} (-1)^{k_3}(m)_{k_3} \left(\frac{\tau_z}{\bar{\gamma}} - \frac{\tau_i}{\bar{\gamma}}\right)^{-m-k_3} \right] & \text{if } m \geq \frac{\mu}{2} \\ \sum\limits_{k_1+\ldots k_3=\omega_i-j} \left[\frac{1}{\prod_{t=1}^{3} k_t!} \prod\limits_{z=1}^{i-1} \frac{(-1)^{k_z}(\omega_z)_{k_z}}{\left(\frac{\tau_z}{\bar{\gamma}} - \frac{\tau_i}{\bar{\gamma}}\right)^{\omega_z+k_z}} \prod\limits_{l=i+1}^{4} \frac{(-1)^{k_{l-1}}(\omega_l)_{k_{l-1}}}{\left(\frac{\tau_l}{\bar{\gamma}} - \frac{\tau_i}{\bar{\gamma}}\right)^{\omega_l+k_{l-1}}} \right] & \text{if } m < \frac{\mu}{2} \end{cases} . \tag{51}$$

$$B_{ij} = \begin{cases} \sum\limits_{\substack{k_1+\ldots k_4=m-j \\ k_1,k_2\leq m-\mu/2}} \left[\frac{(1)_{k_4}}{\prod_{t=1}^{4} k_t!} \left(\frac{-\tau_i}{\bar{\gamma}}\right)^{-(k_4+1)} \prod\limits_{l=1}^{2} \frac{(m-\frac{\mu}{2})!}{(m-\frac{\mu}{2}-k_l)!} \left(\frac{\tau_l}{\bar{\gamma}} - \frac{\tau_i}{\bar{\gamma}}\right)^{m-\frac{\mu}{2}-k_l} \prod\limits_{\substack{z=3 \\ z\neq i}}^{4} \frac{(-1)^{k_3}(m)_{k_3}}{\left(\frac{\tau_z}{\bar{\gamma}} - \frac{\tau_i}{\bar{\gamma}}\right)^{m+k_3}} \right] & \text{if } m \geq \frac{\mu}{2} \\ \sum\limits_{k_1+\ldots k_4=\omega_i-j} \left[\frac{(1)_{k_4}}{\prod_{t=1}^{4} k_t!} \left(\frac{-\tau_i}{\bar{\gamma}}\right)^{-(k_4+1)} \prod\limits_{z=1}^{i-1} \frac{(-1)^{k_z}(\omega_z)_{k_z}}{\left(\frac{\tau_z}{\bar{\gamma}} - \frac{\tau_i}{\bar{\gamma}}\right)^{\omega_z+k_z}} \prod\limits_{l=i+1}^{4} \frac{(-1)^{k_{l-1}}(\omega_l)_{k_{l-1}}}{\left(\frac{\tau_l}{\bar{\gamma}} - \frac{\tau_i}{\bar{\gamma}}\right)^{\omega_l+k_{l-1}}} \right] & \text{if } m < \frac{\mu}{2} \end{cases} . \tag{52}$$

[6] M. D. Yacoub, G. Fraidenraich, H. B. Tercius, and F. C. Martins, "The symmetrical η-κ distribution: a general fading distribution," *IEEE Trans. Broadcast.*, vol. 51, no. 4, pp. 504–511, Dec 2005.

[7] ——, "The asymmetrical η-κ distribution," *Journal of Communication and Information Systems*, vol. 20, no. 3, pp. 182–187, 2005.

[8] M. D. Yacoub, "The α-η-κ-μ fading model," *IEEE Transactions on Antennas and Propagation*, vol. 64, no. 8, pp. 3597–3610, Aug 2016.

[9] M. Yacoub, "The κ-μ distribution and the eta-μ distribution," *IEEE Antennas and Propagation Magazine*, vol. 49, no. 1, pp. 68–81, Feb 2007.

[10] D. Morales-Jimenez and J. F. Paris, "Outage probability analysis for η-μ fading channels," *IEEE Communications Letters*, vol. 14, no. 6, pp. 521–523, June 2010.

[11] N. Ermolova, "Moment Generating Functions of the Generalized η-μ and κ-μ Distributions and Their Applications to Performance Evaluations of Communication Systems," *IEEE Commun. Lett.*, vol. 12, no. 7, pp. 502–504, July 2008.

[12] M. Nakagami, "The m-distribution- a general formula of intensity distribution of rapid fading," *Statistical Method of Radio Propagation*, 1960.

[13] J. F. Paris, "Statistical Characterization of κ-μ Shadowed Fading," *IEEE Trans. Veh. Technol.*, vol. 63, no. 2, pp. 518–526, Feb 2014.

[14] S. L. Cotton, "Human Body Shadowing in Cellular Device-to-Device Communications: Channel Modeling Using the Shadowed κ-μ Fading Model," *IEEE Journal on Selected Areas in Communications*, vol. 33, no. 1, pp. 111–119, Jan 2015.

[15] L. Moreno-Pozas, F. J. Lopez-Martinez, J. F. Paris, and E. Martos-Naya, "The κ-μ shadowed fading model: Unifying the κ-μ and η-μ distributions," *IEEE Trans. Veh. Technol.*, vol. 65, no. 12, pp. 9630–9641, Dec. 2016.

[16] A. Abdi, W. Lau, M.-S. Alouini, and M. Kaveh, "A new simple model for land mobile satellite channels: first- and second-order statistics," *IEEE Trans. Wireless Commun.*, vol. 2, no. 3, pp. 519–528, May 2003.

[17] F. J. Lopez-Martinez, J. F. Paris, and J. M. Romero-Jerez, "The κ-μ shadowed fading model with integer fading parameters," *IEEE Trans. Veh. Technol.*, vol. PP, no. 99, pp. 1–1, 2017.

[18] L. Moreno-Pozas, F. J. Lopez-Martinez, S. L. Cotton, J. F. Paris, and E. Martos-Naya, "Comments on Human Body Shadowing in Cellular Device-to-Device Communications: Channel Modeling Using the Shadowed κ-μ Fading Model," *IEEE J. Sel. Areas Commun.*, vol. 35, no. 2, pp. 517–520, Feb 2017.

[19] A. Erdélyi, *Beitrag zur theorie der konfluenten hypergeometrischen funktionen von mehreren veränderlichen*. Hölder-Pichler-Tempsky in Komm., 1937.

[20] P. W. K. H. M. Srivastava, *Multiple Gaussian Hypergeometric Series*. John Wiley & Sons, 1985.

[21] J. M. Romero-Jerez, F. J. Lopez-Martinez, J. F. Paris, and A. J. Goldsmith, "The Fluctuating Two-Ray Fading Model: Statistical Characterization and Performance Analysis," *to appear in IEEE Trans. Wireless Commun.*, 2017.

[22] E. Martos-Naya, J. M. Romero-Jerez, F. J. Lopez-Martinez, and J. F. Paris, "A MATLAB program for the computation of the confluent hypergeometric function $\Phi 2$," Repositorio Institucional Universidad de Malaga RIUMA., Tech. Rep., 2016.

[23] J. Abate and W. Whitt, "Numerical inversion of Laplace transforms of probability distributions," *ORSA Journal on computing*, vol. 7, no. 1, pp. 36–43, 1995.

[24] J. P. Pena-Martin, J. M. Romero-Jerez, and F. J. Lopez-Martinez, "Generalized MGF of Beckmann Fading With Applications to Wireless Communications Performance Analysis," *IEEE Trans. Commun.*, vol. PP, no. 99, pp. 1–1, 2017.

[25] I. S. Gradshteyn and I. M. Ryzhik, *Table of Integrals, Series and Products*, 7th ed. Academic Press Inc, 2007. [Online]. Available: http://www.worldcat.org/isbn/012294755X

[26] G. D. Durgin, T. S. Rappaport, and D. A. de Wolf, "New analytical models and probability density functions for fading in wireless communications," *IEEE Trans. Comm.*, vol. 50, no. 6, pp. 1005–1015, June 2002.

[27] N. C. Beaulieu and S. A. Saberali, "A generalized diffuse scatter plus line-of-sight fading channel model," in *2014 IEEE International Conference on Communications (ICC)*, June 2014, pp. 5849–5853.

[28] G. L. Stüber, *Principles of mobile communication*. Springer Science & Business Media, 2011.

[29] F. Ramos-Alarcon, V. Kontorovich, and M. Lara, "On the level crossing duration distributions of Nakagami processes," *IEEE Trans. Commun.*, vol. 57, no. 2, pp. 542–552, February 2009.

[30] F. J. López-Martínez, E. Martos-Naya, J. F. Paris, and U. Fernández-Plazaola, "Higher Order Statistics of Sampled Fading Channels With Applications," *IEEE Trans. Veh. Technol.*, vol. 61, no. 7, pp. 3342–3346, Sept 2012.

[31] S. L. Cotton and W. G. Scanlon, "Higher-order statistics for κ-μ distribution," *Electronics Letters*, vol. 43, no. 22, Oct 2007.

[32] A. V. Oppenheim, A. S. Willsky, and S. H. Nawab, *Signals & Systems (2Nd Ed.)*. Prentice-Hall, Inc., 1996.

Pablo Ramirez-Espinosa received the M.Sc. degree in electrical engineering from the University of Málaga, Málaga, Spain, in 2017, where he has been working toward the Ph.D. degree in communication theory. Since 2017, he has been with the Communication Engineering Department, University of Málaga, as an Associate Researcher. His main research activities are in wireless communications, particularly channel modeling.

Copyright (c) 2018 IEEE. Personal use is permitted. For any other purposes, permission must be obtained from the IEEE by emailing pubs-permissions@ieee.org.

This is the author's version of an article that has been published in this journal. Changes were made to this version by the publisher prior to publication.
The final version of record is available at http://dx.doi.org/10.1109/TVT.2017.2787204

F. Javier Lopez-Martinez received the M.Sc. and Ph.D. degrees in telecommunication engineering from the Universidad de Malaga, Spain, in 2005 and 2010, respectively. He joined the Communication Engineering Department with the Universidad de Malaga in 2005, as an Associate Researcher. In 2010, he stayed for three months as a Visitor Researcher with University College London. He was a Marie Curie Post-Doctoral Fellow with the Wireless Systems Lab, Stanford University, from 2012 to 2014, and with the Universidad de Malaga from 2014 to 2015. Since 2015, he has been an Assistant Professor with the Communication Engineering Department, Universidad de Malaga. His research interests span a diverse set of topics in the wide areas of communication theory and wireless communications: stochastic processes, wireless channel modeling, random matrix theory, physical layer security, massive MIMO, and mmWave for 5G. He has received several research awards, including the Best Paper Award in the Communication Theory Symposium at IEEE Globecom 2013, the IEEE Communications Letters Exemplary Reviewer certificate in 2014, and the IEEE Transactions on Communications Exemplary Reviewer certificate in 2015 and 2017. He is an Editor of the IEEE Transactions on Communications, in the area of Wireless Communications, and a Senior Member of the IEEE.

José F. Paris received the M.Sc. and Ph.D. degrees in telecommunication engineering from the Universidad de Málaga, Spain, in 1996 and 2004, respectively. From 1994 to 1996 he was with Alcatel, mainly in the development of wireless telephones. In 1997, he joined the Universidad de Málaga, where is currently a Professor with the Communication Engineering Department. His teaching activities include several courses on digital communications, signal processing, and acoustic engineering. His research interests are related to wireless communications, especially channel modeling, and performance analysis. In 2005, he spent five months as a Visiting Associate Professor with Stanford University, with Prof. A. J. Goldsmith. From 2017 he is Full Professor with the Communication Engineering Department. He received the 2016 Neil Shepherd Memorial Best Propagation Paper Award by the IEEE Vehicular Technology Society. He serves as an Associate Editor of the IEEE Communications Letters, and the IEEE Transactions on Vehicular Technology.

Michel Daoud Yacoub was born in Brazil in 1955. He received the B.S.E.E. and M.Sc. degrees from the School of Electrical and Computer Engineering of the State University of Campinas, UNICAMP, Campinas, SP, Brazil, in 1978 and 1983, respectively, and the Ph.D. degree from University of Essex, U.K., in 1988. From 1978 to 1985, he worked as a Research Specialist in the development of the Tropico digital exchange family with the Research and Development Center of Telebrs, Brazil. In 1989, he joined the School of Electrical and Computer Engineering, UNICAMP, where he is currently a Full Professor. He consults for several operating companies and industries in the wireless communications area. He is the author of Foundations of Mobile Radio Engineering (Boca Raton, FL: CRC, 1993), Wireless Technology: Protocols, Standards, and Techniques (Boca Raton, FL: CRC, 2001), and the coauthor of Telecommunications: Principles and Trends (So Paulo, Brasil: Erica, 1997, in Portuguese). He holds two patents. His general research interests include wireless communications.

Eduardo Martos-Naya received the M.Sc. and Ph.D. degrees in telecommunication engineering from the University of Málaga, Málaga, Spain, in 1996 and 2005, respectively. In 1997, he joined the Department of Communication Engineering, University of Málaga, where he is currently an Associate Professor. His research activity includes digital signal processing for communications, synchronization and channel estimation, and performance analysis of wireless systems. Currently, he is the leader of a project supported by the Andalusian regional Government on cooperative and adaptive wireless communications systems.

Copyright (c) 2018 IEEE. Personal use is permitted. For any other purposes, permission must be obtained from the IEEE by emailing pubs-permissions@ieee.org.